Direct evidence for orientational flip-flop of water molecules at charged interfaces: A heterodyne-detected vibrational sum frequency generation study

Cite as: J. Chem. Phys. **130**, 204704 (2009); https://doi.org/10.1063/1.3135147
Submitted: 15 February 2009 • Accepted: 24 April 2009 • Published Online: 26 May 2009

Satoshi Nihonyanagi (二本柳聡史), **Shoichi Yamaguchi** (山口祥一) **and Tahei Tahara** (田原太平)

Direct evidence for orientational flip-flop of water molecules at charged interfaces: A heterodyne-detected vibrational sum frequency generation study

Satoshi Nihonyanagi (二本柳聡史), Shoichi Yamaguchi (山口祥一), and Tahei Tahara (田原太平)[a)]
Molecular Spectroscopy Laboratory, Advanced Science Institute (ASI), RIKEN, 2-1 Hirosawa, Wako, Saitama 351-0198, Japan

(Received 15 February 2009; accepted 24 April 2009; published online 26 May 2009)

Complex $\chi^{(2)}$ spectra of air/water interfaces in the presence of charged surfactants were measured by heterodyne-detected broadband vibrational sum frequency generation spectroscopy for the first time. In contrast to the neat water surface, the signs of $\chi^{(2)}$ for two broad OH bands are the same in the presence of the charged surfactants. The obtained $\chi^{(2)}$ spectra clearly showed flip-flop of the interfacial water molecules which is induced by the opposite charge of the head group of the surfactants. With the sign of $\beta^{(2)}$ theoretically obtained, the absolute orientation, i.e., up/down orientation, of water molecules at the charged aqueous surfaces was uniquely determined by the relation between the sign of $\chi^{(2)}$ and the molecular orientation angle. Water molecules orient with their hydrogen up at the negatively charged aqueous interface whereas their oxygen up at the positively charged aqueous interface. © *2009 American Institute of Physics*.
[DOI: 10.1063/1.3135147]

Understanding of the water structure at charged interfaces is critically important in the wide range of scientific fields such as biophysics, colloid science, and electrochemistry. Among various interactions between a charged interface and water molecules, charge-dipole interaction is often a predominant factor to determine the water structure at the interface.[1] When an aqueous interface is positively charged and the surface charge density is sufficiently high, one expects that water molecules point their oxygen up to the positively charged interface. On the other hand, one expects water molecules orient with their hydrogen up at a negatively charged interface. This is the so-called flip-flop model of interfacial water molecules.[1] However, direct spectroscopic evidence for such a fundamental picture has not been reported due to the lack of a methodology to unambiguously determine absolute, i.e., "up/down," orientation of molecules at interfaces.

Interface-selective vibrational sum frequency generation (VSFG) spectroscopy is a powerful tool to identify surface species and determine their orientational angles.[2–6] Furthermore, the second-order nonlinear susceptibility ($\chi^{(2)}$) intrinsically contains information about the absolute orientation of surface species in its sign. However, the information of the sign (or phase) of $\chi^{(2)}$ is lost in the conventional (homodyne-detected) VSFG spectroscopy that detects the intensity of the sum frequency (SF) light, i.e., a square of the SF field. Thus, the absolute orientation of the surface species cannot be determined by the usual homodyne-detected VSFG spectroscopy.

To obtain the sign of $\chi^{(2)}$, the heterodyne detection can be applied to VSFG. The heterodyne-detected VSFG is very powerful, but the number of reports is very limited because of technical difficulty. Shen and co-workers[7–10] first reported phase-sensitive VSFG that can provide the real and imaginary parts of $\chi^{(2)}$. Their method is based on the single-channel detection with a narrow-band IR laser scanned in a spectral range, which results in a long measurement time. Stiopkin *et al.*[11] recently demonstrated the heterodyne detection of multiplex (broadband) VSFG. They showed significant improvement in detection sensitivity, but did not determine the real and imaginary parts of $\chi^{(2)}$ separately, probably because of the phase instability.

In the present work, we report development of multiplex heterodyne-detected VSFG (HD-VSFG) that can provide the real and imaginary parts of $\chi^{(2)}$ and its application to aqueous interfaces. Our HD-VSFG is technically based on the heterodyne-detected multiplex electronic sum frequency generation recently developed by us.[12] Our method has a great advantage in the phase stability, which allows us to measure complex $\chi^{(2)}$ spectra, and in the short acquisition time as well. The complex $\chi^{(2)}$ spectra of water at the interfaces were measured in the presence of prototypical charged surfactants, sodium dodecyl sulfate (SDS), and cetyltrimethylammonium bromide (CTAB). The absolute orientation of water molecules at the simple model interfaces charged with the surfactants was directly determined by the measurement of $\chi^{(2)}$, for the first time.

The essential part of the optical configuration of HD-VSFG is depicted in Fig. 1(a). Two-thirds of the output from a regenerative amplifier (Spectra Physics, Spitfire Pro XP; ~3.3 W, 1 kHz) was used for excitation of a commercial optical parametric amplifier and a difference frequency gen-

[a)]Author to whom correspondence should be addressed. Tel.: (+81) 48-467-7928. FAX: (+81) 48-467-4539. Electronic mail: tahei@riken.jp.

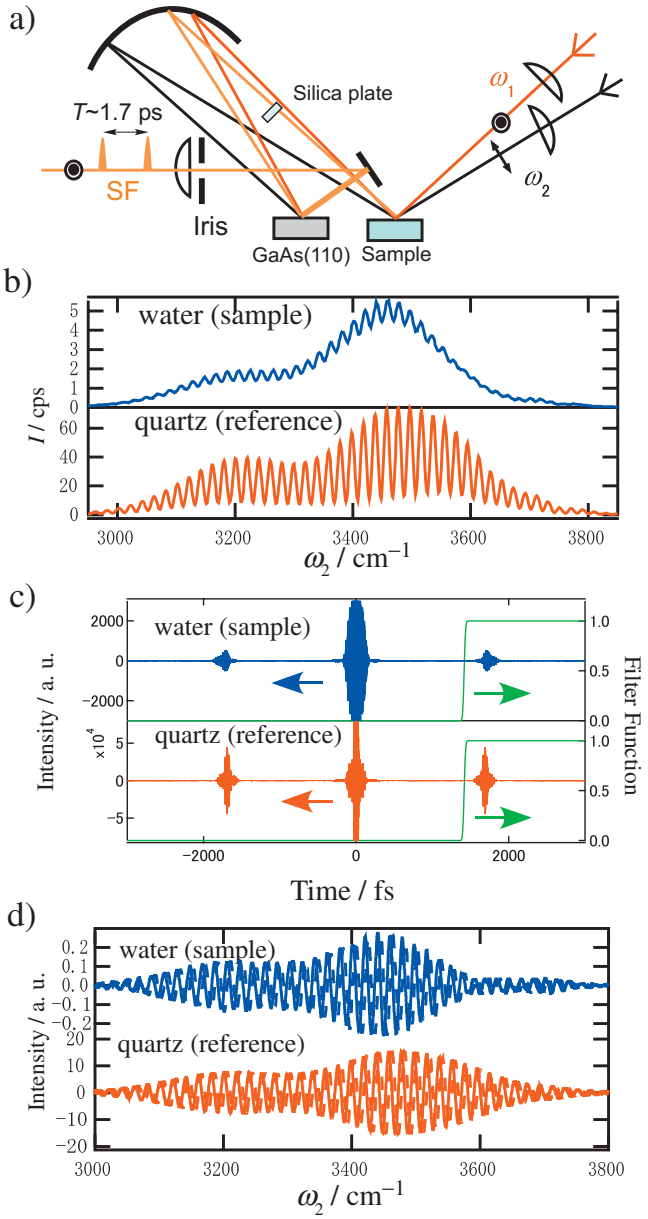

FIG. 1. (Color) (a) The optical configuration of the HD-VSFG measurements. (b) Raw spectra of the air/water interface (blue) and z-cut quartz crystal (red). (c) Time domain interferogram (blue and red) and the filter function (green). (d) Real (solid lines) and imaginary (dashed lines) parts of the filtered heterodyne spectra of the sample and reference.

erator (Spectra Physics, TOPAS C & DFG1) to generate broadband IR (ω_2, center wavelength: 2900 nm, bandwidth: ~500 cm^{-1}, average power: 18 mW). The spectrum of this broadband ω_2 pulse covers the whole frequency region of the OH stretching vibration of water (~800 cm^{-1}) without scanning the ω_2 center wavelength. The rest of the regenerative amplifier output was used as the visible (ω_1) light for the HD-VSFG measurement after passing through a narrowband filter [CVI Melles Griot, center wavelength: 795 nm, bandwidth: 1.5 nm (24 cm^{-1})]. The average power of the ω_1 beam was 6.3 mW at the sample position. The ω_1 and ω_2 beams are spatially and temporally overlapped on a sample surface with incident angles of 44° and 59°, respectively, to generate the SF at $\omega_1+\omega_2$. The ω_1, ω_2, and SF beams reflected by the sample surface are refocused by a concave mirror onto a GaAs(110) surface to generate another SF that acts as a local oscillator (LO). In this arrangement, the optical path length of the SF pulse from the sample surface to the GaAs surface has exactly the same fluctuation as that of ω_1 and ω_2 pulses, which keeps relative phase between the two SF pulses (i.e., the sample signal and LO) stable for at least a few hours. The SF pulse from the sample passes through a 1 mm thick silica plate located in between the sample and the concave mirror, which delays the SF pulse relative to the ω_1 and ω_2 pulses by T (=1.7 ps). This delay generates the time difference between the SF pulse from the sample and that from the GaAs. The two SF beams are introduced together into a polychromator and then detected by charge coupled device (CCD). In the polychromator, the two SF pulses are stretched in time and interfere to generate an interference pattern in the frequency domain. The SF, ω_1, and ω_2 beams were *s*-, *s*-, and *p*-polarized, respectively, (*ssp* polarization combination) in the present study. A typical CCD exposure time was 2 min and each spectrum presented is an average of two exposures. SDS (Aldrich) and CTAB (Wako) were used as received. The surfactants were dissolved in purified water (Millipore, 18.2 MΩ cm resistivity) and each solution was filled in clean glass containers. The height of the aqueous surface was monitored by a displacement sensor (Keyence, LK-G150) and kept to be the same as the height of a reference *z*-cut quartz crystal surface with accuracy of a few microns. This is critical for the accurate phase measurement. The quartz crystal was purchased from Furuuchi Chemical and piezoelectric measurement data were supplied by the vendor.

Figure 1(b) shows a raw HD-VSFG spectrum of the air/water interface measured with the present setup. The detected total intensity [I, Fig. 1(b)] is represented as[12]

$$I = |\tilde{E}_{\mathrm{tot}}(\omega)|^2 = |\tilde{E}_{\mathrm{sample}}|^2 + |\tilde{E}_{\mathrm{LO}}|^2 + \tilde{E}_{\mathrm{sample}}\tilde{E}^*_{\mathrm{LO}} \exp(i\omega T) + \tilde{E}^*_{\mathrm{sample}}\tilde{E}_{\mathrm{LO}} \exp(-i\omega T). \quad (1)$$

Here, $\tilde{E}_{\mathrm{sample}}$ and $\tilde{E}_{\mathrm{LO}}$ denote the SF electric fields from the sample and GaAs, respectively, in the frequency domain. The cross terms, $\tilde{E}_{\mathrm{sample}}\tilde{E}^*_{\mathrm{LO}} \exp(i\omega T)$ and $\tilde{E}^*_{\mathrm{sample}}\tilde{E}_{\mathrm{LO}} \exp(-i\omega T)$, correspond to the fringe structure that contains the phase information. The raw spectrum is inverse-Fourier-transformed into the time domain, as shown in Fig. 1(c), where the two cross terms, $\tilde{E}_{\mathrm{sample}}\tilde{E}^*_{\mathrm{LO}} \exp(i\omega T)$ and $\tilde{E}^*_{\mathrm{sample}}\tilde{E}_{\mathrm{LO}} \exp(-i\omega T)$, give the peaks at $t=1.7$ ps and -1.7 ps, respectively. The peak at $t=0$ ps is due to $|\tilde{E}_{\mathrm{sample}}|^2$ and $|\tilde{E}_{\mathrm{LO}}|^2$. Because the three peaks in the time-domain interferogram are well separated, the peak at $t=1.7$ ps can be picked up by applying a filter function depicted in Fig. 1(c). This filtering of the time-domain interferogram followed by the Fourier transformation back into the frequency domain gives the complex spectrum of $\tilde{E}_{\mathrm{sample}}\tilde{E}^*_{\mathrm{LO}} \exp(i\omega T)$, as shown in Fig. 1(d). Similarly, a HD-VSFG spectrum was measured from the z-cut quartz with the same GaAs [Figs. 1(b)–1(d), red curves]. The quartz does not have any resonance so that the quartz spectrum can be used as a reference. Consequently, the real and imaginary $\chi^{(2)}$ spectra of the sample (Fig. 2) can be obtained by dividing the sample in-

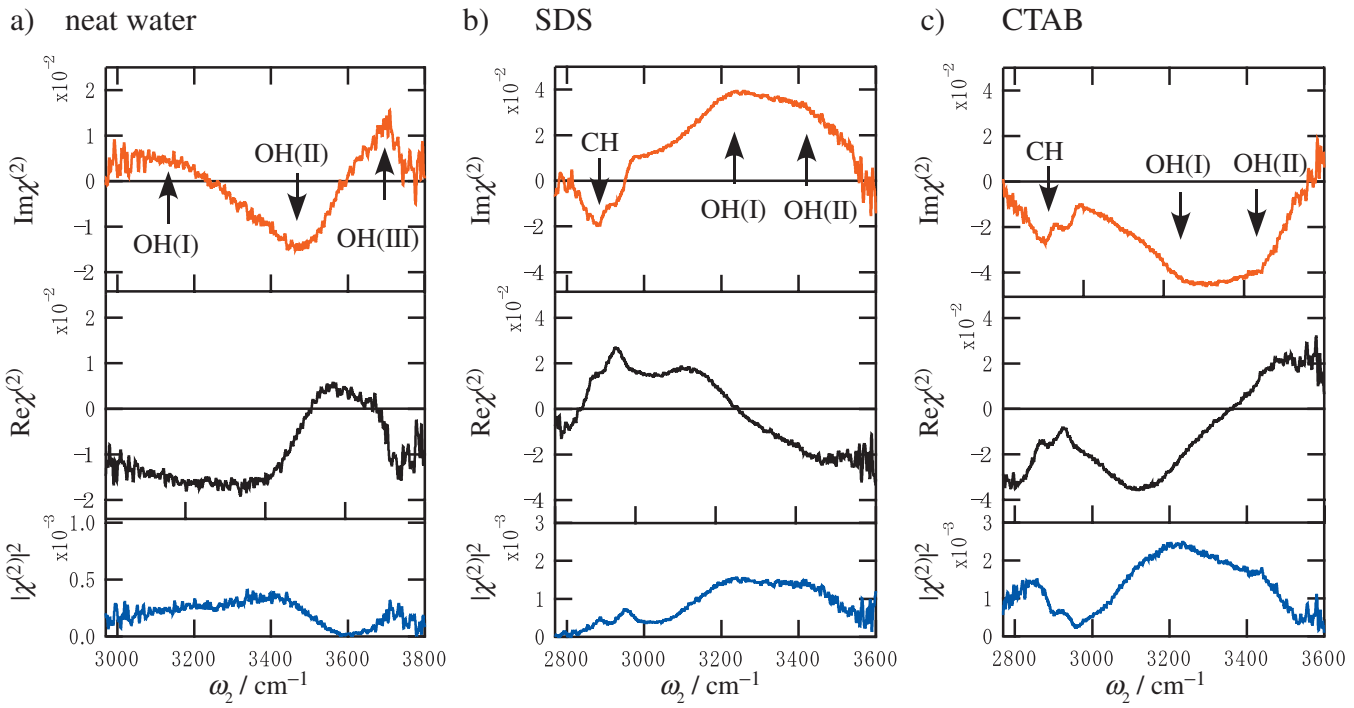

FIG. 2. (Color) Im $\chi^{(2)}$ (red), Re $\chi^{(2)}$ (black), and $|\chi^{(2)}|^2$ (blue) spectra of (a) neat water/air, (b) SDS solution/air, and (c) CTAB solution/air interfaces. OH(I), OH(II), and OH(III) represent the three characteristic bands in the OH stretching region. CH stands for the CH_3 stretching band of the surfactants. χ^{NR} appeared in Re $\chi^{(2)}$ in the negative side, corresponding to the phase being $\pi \pm 0.1\pi$.

terferogram [Fig. 1(d), blue curves] by the quartz reference interferogram [Fig. 1(d), red curves]. $\chi^{(2)}$ in the *ssp* polarization combination is given by the following equation:[12,13]

$$\chi^{(2)} \equiv \frac{F_{\text{sample}} r_{1,\text{sample}} r_{2,\text{sample}}}{F_{\text{quartz}} r_{1,\text{quartz}} r_{2,\text{quartz}}} \frac{\chi^{(2)}_{yyz,\text{sample}}}{\chi^{(2)}_{yyz,\text{quartz}}}, \tag{2}$$

where F is the product of Fresnel factors (L) for SF, ω_1 and ω_2, with the given polarizations; $F=AL_{\text{SF}}L_1L_2$, where A is a positive real constant. In the *ssp* polarization combination, F_{sample} and F_{quartz} are all positive. $r_{j,X}$ is a complex reflectivity for the ω_j electric field at the surface X, i.e., sample or quartz. This quantity appears in this formula because E_{LO} is generated by the ω_1 and ω_2 beams that are reflected from the sample or quartz surface. $r_{1,\text{sample}}r_{2,\text{sample}}/r_{1,\text{quartz}}r_{2,\text{quartz}}$ is real and positive.[14] The subscripts of $\chi^{(2)}_{yyz}$ in Eq. (2) stand for the laboratory axes. The z axis is parallel to the surface normal and the y axis is parallel to the s polarization. $\chi^{(2)}_{yyz,\text{quartz}}$ is a real constant over the spectral range and the sign of $\chi^{(2)}_{yyz,\text{quartz}}$ is determined to be positive from the piezoelectric data. Therefore, the sign of $\chi^{(2)}$ simply reflects the sign of $\chi^{(2)}_{yyz,\text{sample}}$ of the aqueous surfaces. As clearly shown in Eq. (2), E_{LO} is completely canceled out. Thus, any dispersion of GaAs does not affect the normalized $\chi^{(2)}$ spectra.

Figure 2 shows the Im $\chi^{(2)}$ (imaginary part of $\chi^{(2)}$), Re $\chi^{(2)}$ (real part of $\chi^{(2)}$), and $|\chi^{(2)}|^2$ spectra of air/aqueous interfaces for (a) neat water, (b) 10 mM SDS solution, and (c) 10 mM CTAB solution. ($|\chi^{(2)}|^2$ spectra were calculated from the measured Im $\chi^{(2)}$ and Re $\chi^{(2)}$.) Im $\chi^{(2)}$ spectra are directly associated with the vibrational resonance and thus most informative. The $\chi^{(2)}$ spectra of the neat water surface [Fig. 2(a)] are essentially the same as that reported by Ji *et al.*[10] very recently. The broad positive band around 3200 cm^{-1} [OH(I)] in the Im $\chi^{(2)}$ spectrum is often assigned to the symmetric OH stretching of tetrahedrally hydrogen bonded water (icelike water) and a negative band around 3450 cm^{-1} [OH(II)] to symmetric stretching (ss) of asymmetrically hydrogen bonded water (liquidlike water).[15] It was also pointed out that Fermi resonance splitting of the OH symmetric stretch band contributes spectral feature in this region.[16,17] In either case, both of the 3200 and 3450 cm^{-1} bands observed in the *ssp* polarization combination were assigned to the symmetric OH stretch, not to the antisymmetric stretch.[18] This assignment is a basis of the orientation analysis described below. A characteristic sharp band at 3700 cm^{-1} [OH(III)] is assigned to "free OH" of water at the topmost surface layer.[15]

The negative features observed at 2880 and 2940 cm^{-1} in the Im $\chi^{(2)}$ spectrum of the SDS aqueous solution/air interface [Fig. 2(b)] are assigned to the ss of the terminal CH_3 of SDS and its Fermi resonance, broadened by shoulders associated with symmetric and antisymmetric CH_2 stretching of the SDS hydrocarbon chain.[19] At this concentration, the adsorption of SDS at the aqueous surface is saturated.[20] The Im $\chi^{(2)}$ signals above 3000 cm^{-1} in Fig. 2(b) are all due to the OH stretching of water molecules near the negatively charged SDS/water interface. The charge of the head group of SDS affects the water structure significantly. Unlike the neat water surface[10] [Fig. 2(a)], both of the OH(I) and OH(II) bands are positive at the SDS/water interface, which demonstrates that relevant transition moments of water vibrations align toward the same side. Because both bands originate from the symmetric OH stretch, this supports the idea that the electric field determines the water orientation at this model interface. In addition, the intensity of the hydrogen

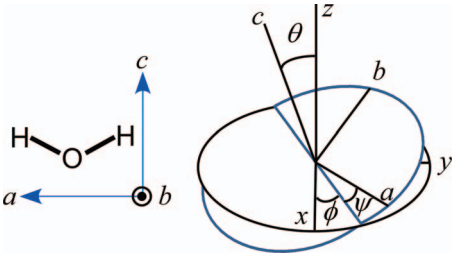

FIG. 3. (Color) Definition of the molecular-frame coordinates of water (a,b,c), the laboratory-frame coordinates (x,y,z), and the Euler angles (θ,ψ,ϕ). The c axis is set to be the bisector of the angle of H–O–H that is placed on the ac plane.

bonded OH bands are enhanced at the charged interfaces compared to the neat water whereas the free OH band vanishes, being consistent with previous VSFG studies.[21,22]

The Im $\chi^{(2)}$ spectrum of CTAB [Fig. 2(c)] exhibits broad OH bands having the negative sign. This is the direct evidence for the flip-flop of water molecules, i.e., the orientation of water molecule at the positively charged interface is opposite to that at the negatively charged one. Similar phase difference by π has been suggested by earlier works involving the fitting of homodyne VSFG spectra of aqueous interfaces.[23–25]

These HD-VSFG spectra not only demonstrate the flip-flop of interfacial water molecules but also can determine the absolute orientation, i.e., orientation with respect to the laboratory frame, of the water molecules. To do this, the relation between $\chi^{(2)}_{yyz,\mathrm{sample}}$ and the orientation angle of water molecule (θ) needs to be derived. $\chi^{(2)}_{yyz,\mathrm{sample}}$ in the laboratory coordinate consists of a vibrationally nonresonant $(\chi^{\mathrm{NR}}_{yyz})$ and resonant terms and can be represented as follows:

$$\chi^{(2)}_{yyz,\mathrm{sample}} = \chi^{\mathrm{NR}}_{yyz} + \sum_q \frac{\chi^q_{yyz}}{\omega_q - \omega_2 - i\Gamma_q}. \tag{3}$$

Here, the Lorenzian band shape is assumed for vibrational resonant terms. χ^{NR}_{yyz} and χ^q_{yyz} are real under the present electronically nonresonant condition. Γ_q is a real positive damping constant. The sign of Im $\chi^{(2)}_{yyz,\mathrm{sample}}$ is that of χ^q_{yyz}. A tensor element of the molecular hyperpolarizability in the molecular coordinate $\beta^{(2)}_{ijk}$ relates to its amplitude β_{ijk} in the same manner,

$$\beta^{(2)}_{ijk} = \beta^{\mathrm{NR}}_{ijk} + \sum_q \frac{\beta_{ijk}}{\omega_q - \omega_2 - i\Gamma_q}. \tag{4}$$

According to literature by Gan *et al.*,[18] χ^q_{yyz} of isotropic aqueous surfaces can be written for the OH ss mode as follows:

$$\chi^{\mathrm{OHss}}_{yyz} = \frac{1}{2}N_s\{(\langle\cos^2\psi\rangle\beta_{aac} + \langle\sin^2\psi\rangle\beta_{bbc} + \beta_{ccc})\langle\cos\theta\rangle + (\langle\sin^2\psi\rangle\beta_{aac} + \langle\cos^2\psi\rangle\beta_{bbc} - \beta_{ccc})\langle\cos^3\theta\rangle\}, \tag{5}$$

where N_s is the number of surface water molecules and the brackets stand for ensemble average. The Euler angles (θ,ψ,ϕ) and the molecular axes (a,b,c) were defined as shown in Fig. 3. In this system, θ is the orientation angle, i.e., the angle between the molecular c axis and the surface normal. The c axis corresponds to the direction of the transition dipole moment of the symmetric OH stretching vibration of water. The azimuthal angle ϕ is randomly distributed at an isotropic liquid surface. Morita and Hynes[26] calculated the derivatives of the dipole moment and polarizability with respect to the OH vibration and showed that β_{aac}, β_{bbc}, and β_{ccc} are all positive. The relative β_{ijk} values for the symmetric OH stretching of water molecule were given by Gan *et al.*[18] as follows: $\beta_{aac}=1.296$, $\beta_{bbc}=0.557$, and $\beta_{ccc}=1$. Consequently, introducing these values to Eq. (5), we obtain

$$\chi^{\mathrm{OHss}}_{yyz} = \frac{1}{2}N_s\beta_{ccc}\left\{\left(1.296 + 0.557\frac{\langle\cos^3\theta\rangle}{\langle\cos\theta\rangle}\right)\langle\cos^2\psi\rangle + \left(0.557 + 1.296\frac{\langle\cos^3\theta\rangle}{\langle\cos\theta\rangle}\right)\langle\sin^2\psi\rangle + \left(1 - \frac{\langle\cos^3\theta\rangle}{\langle\cos\theta\rangle}\right)\right\}\langle\cos\theta\rangle. \tag{6}$$

Because $\langle\cos^3\theta\rangle/\langle\cos\theta\rangle > 0$, $\langle\cos^2\psi\rangle > 0$, $\langle\sin^2\psi\rangle > 0$, and $(1-\langle\cos^3\theta\rangle/\langle\cos\theta\rangle) > 0$, $\chi^{\mathrm{OHss}}_{yyz}$ is positive when $\langle\cos\theta\rangle > 0$ whereas it is negative when $\langle\cos\theta\rangle < 0$. This relation is experimentally confirmed by the fact that the free OH, which is expected to have $\langle\cos\theta\rangle > 0$, was observed as a positive band in Fig. 2(a). Morita and Hynes[26] calculated $\chi^{\mathrm{OHss}}_{yyz}$ as a function of cos θ using molecular dynamics simulation and gave the same conclusion. Note that this analysis on the absolute orientation is applicable to any molecules if β_{ijk} and symmetry are known.

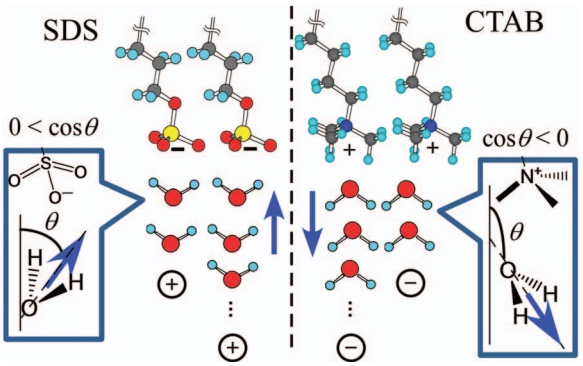

FIG. 4. (Color) Sketch for the SDS and CTAB solutions/air interfaces. The orientation angle θ is defined as the angle between the transition dipole moment of the symmetric OH stretching and the surface normal. The circles with + or − represent counter ions in solutions.

Based on the above-mentioned relation between $\chi^{\mathrm{OHss}}_{yyz}$ and θ, we can conclude that the positive Im $\chi^{(2)}$ of the OH bands for the SDS solution indicates that water molecules orient with their hydrogen up toward the negative charge in the SDS head group. On the other hands, the negative Im $\chi^{(2)}$ of the OH bands for the CTAB solution indicates that water molecules orient with their hydrogen down pointing away from the positive charge in the CTAB head group (Fig. 4). These results agree well with the structure that has been expected, but has not been directly proved, in the flip-flop model for the charged aqueous interfaces.

The intensity of the OH bands at the charged interfaces is enhanced compared to the neat water owing to the effect

of the surface electric field. The saturated surface density of SDS was reported to be as high as 2 molecules/nm^2.[20] Therefore the surface charge density is $2e/\mathrm{nm}^2$ (e is the elementary charge). It has been suggested that the surface electric field aligns the water molecules near the surface, which causes larger $\chi^{(2)}$.[21,27] The thickness of the water layers oriented by the surface electric field was simulated to be larger than the thickness of the oriented water layer at the neutral surface,[28] where only two or three layers of water molecules are oriented.[26] The thickness of oriented water layer is approximated, at a maximum, by the thickness of the Gouy–Chapman layer (3 nm), which corresponds to approximately ten water layers for 10 mM monovalent ions.[23,29] In addition, the absence of the destructive interference between the OH(I) and OH(II) bands at the charged interface seems to also contribute to the intensity enhancement.

The shape of the CH bands of CTAB and SDS are essentially the same, except the vertical shift due to the long tail of the OH band [Figs. 2(b) and 2(c)]. This indicates that the arrangement of the CTAB hydrocarbon chain is very similar to that of SDS at the two interfaces. The relation between $\chi_{yyz}^{\mathrm{CHss}}$ and the orientation angle of the methyl group is similar to Eq. (6) (Ref. 30) but β_{ccc} is negative.[31,32] Thus, the observed negative CH bands indicate that the terminal methyl group is aligned toward the air side, as it is expected. The fact that the CH bands were observed as negative bands in both Figs. 2(b) and 2(c) confirms that there was no erratic phase shift between the measurements of the two different interfaces.

The $|\chi^{(2)}|^2$ spectra in Figs. 2(b) and 2(c) agree well with VSFG spectra of SDS and decylammonium chloride solution, respectively, reported by Gragson *et al.*[21] The $|\chi^{(2)}|^2$ spectra exhibit smaller CH and OH bands for SDS [Fig. 2(b)] and larger CH and OH bands for CTAB [Fig. 2(c)]. It is because the $\chi_{yyz}^{\mathrm{OHss}}$ interferes with the $\chi_{yyz}^{\mathrm{CHss}}$ and χ_{yyz}^{NR}, destructively for SDS and constructively for CTAB.[21] The Im $\chi^{(2)}$ spectra are free from such complexity due to interference arising from squaring. This is another notable advantage of $\chi^{(2)}$ spectra over $|\chi^{(2)}|^2$ spectra.

This work was financially supported by a Grant-in-Aid for Scientific Research on Priority Area "Molecular Science for Supra Functional Systems" (No. 19056009) from MEXT and a Grant-in-Aid for Scientific Research (A) (No. 19205005) from JSPS. S.N. acknowledges the Special Postdoctoral Researchers Program of RIKEN.

[1] J. O. M. Bockris and A. K. N. Reddy, *Modern Electrochemistry 2A: Fundamentals of Electronics*, 2nd ed. (Plenum, New York, 2001).
[2] Y. R. Shen, *The Principles of Nonlinear Optics* (Wiley, New York, 1984).
[3] Y. R. Shen, Nature (London) **337**, 519 (1989).
[4] C. D. Bain, J. Chem. Soc., Faraday Trans. **91**, 1281 (1995).
[5] C. Hirose, N. Akamatsu, and K. Domen, J. Chem. Phys. **96**, 997 (1992).
[6] J. Holman, P. B. Davies, T. Nishida, S. Ye, and D. J. Neivandt, J. Phys. Chem. B **109**, 18723 (2005).
[7] R. Superfine, J. Y. Huang, and Y. R. Shen, Opt. Lett. **15**, 1276 (1990).
[8] V. Ostroverkhov, G. A. Waychunas, and Y. R. Shen, Chem. Phys. Lett. **386**, 144 (2004).
[9] N. Ji, V. Ostroverkhov, C. Y. Chen, and Y. R. Shen, J. Am. Chem. Soc. **129**, 10056 (2007).
[10] N. Ji, V. Ostroverkhov, C. S. Tian, and Y. R. Shen, Phys. Rev. Lett. **100**, 096102 (2008).
[11] I. V. Stiopkin, H. D. Jayathilake, A. N. Bordenyuk, and A. V. Benderskii, J. Am. Chem. Soc. **130**, 2271 (2008).
[12] S. Yamaguchi and T. Tahara, J. Chem. Phys. **129**, 101102 (2008).
[13] i in front of E_{quartz} is needed to compensate the phase difference between surface and bulk SFG. See Ref. 12 for detail.
[14] In a strict sense, $L_{2,\mathrm{sample}}$ or $r_{2,\mathrm{sample}}$ is not constant but dependent on ω_2 in the OH stretching region because of the vibrational resonance. According to the calculation of the complex Fresnel factor and reflectivity, the phase shifts due to $L_{2,\mathrm{sample}}$ and $r_{2,\mathrm{sample}}$ are $\sim\pi/10$, which is about the size of experimental uncertainty of the phase. Thus, we limit our discussion to a large phase shift (π). The present $\chi^{(2)}$ spectra were not normalized to the ω_2 dependence of $L_{2,\mathrm{sample}}$ and $r_{2,\mathrm{sample}}$.
[15] Q. Du, R. Superfine, E. Freysz, and Y. R. Shen, Phys. Rev. Lett. **70**, 2313 (1993).
[16] W. F. Murphy and H. J. Bernstein, J. Phys. Chem. **76**, 1147 (1972).
[17] M. Sovago, R. K. Campen, G. W. H. Wurpel, M. Muller, H. J. Bakker, and M. Bonn, Phys. Rev. Lett. **101**, 139402 (2008).
[18] W. Gan, D. Wu, Z. Zhang, R. Feng, and H. Wang, J. Chem. Phys. **124**, 114705 (2006).
[19] J. C. Conboy, M. C. Messmer, and G. L. Richmond, J. Phys. Chem. B **101**, 6724 (1997).
[20] T. Kawai, H. Kamio, T. Kondo, and K. Kon-No, J. Phys. Chem. B **109**, 4497 (2005).
[21] D. E. Gragson, B. M. McCarty, and G. L. Richmond, J. Am. Chem. Soc. **119**, 6144 (1997).
[22] Q. Du, E. Freysz, and Y. R. Shen, Phys. Rev. Lett. **72**, 238 (1994).
[23] D. E. Gragson and G. L. Richmond, J. Phys. Chem. B **102**, 3847 (1998).
[24] M. S. Yeganeh, S. M. Dougal, and H. S. Pink, Phys. Rev. Lett. **83**, 1179 (1999).
[25] S. Ye, S. Nihonyanagi, and K. Uosaki, Phys. Chem. Chem. Phys. **3**, 3463 (2001).
[26] A. Morita and J. T. Hynes, Chem. Phys. **258**, 371 (2000).
[27] X. Chen, T. Yang, S. Kataoka, and P. S. Cremer, J. Am. Chem. Soc. **129**, 12272 (2007).
[28] K. J. Schweighofer, X. Xia, and M. L. Berkowitz, Langmuir **12**, 3747 (1996).
[29] The bulk concentration of the "free" counterion is ~2 mM for 10 mM CTAB due to the micellization. [T. Asakawa, H. Kitano, A. Ohta, and S. Miyagishi, J. Colloid Interface Sci. **242**, 284 (2001).] The corresponding thickness of Gouy-Chapman layer is 6.9 nm.
[30] C. Hirose, N. Akamatsu, and K. Domen, Appl. Spectrosc. **46**, 1051 (1992).
[31] K. B. Wiberg and J. J. Wendoloski, J. Phys. Chem. **88**, 586 (1984).
[32] M. Oh-e, A. I. Lvovsky, X. Wei, and Y. R. Shen, J. Chem. Phys. **113**, 8827 (2000); note that the sign of β is opposite to ours in their paper because of the different sign of the denominator in Eq. (4).